

Live Imaging of Cellular Internalization of Single Colloidal Particle by Combined Label-Free and Fluorescence Total Internal Reflection Microscopy

Gerard D. Byrne,^{†,‡,||} Driton Vllasaliu,^{†,§} Franco H. Falcone,[§] Michael G. Somekh,^{‡,#} and Snjezana Stolnik^{*,†}

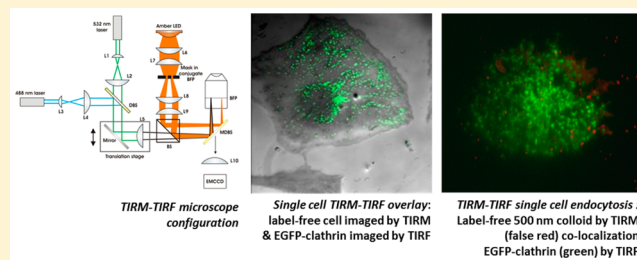
[†]Drug Delivery and Tissue Engineering Division, School of Pharmacy, University of Nottingham, Nottingham, NG7 2RD, U.K.

[‡]Institute of Biophysics, Imaging and Optical Science (IBIOS), School of Electrical and Electronic Engineering, University of Nottingham, Nottingham, NG7 2RD, U.K.

[§]Division of Molecular and Cellular Science, School of Pharmacy, University of Nottingham, Nottingham, NG7 2RD, U.K.

ABSTRACT: In this work we utilize the combination of label-free total internal reflection microscopy and total internal reflectance fluorescence (TIRM/TIRF) microscopy to achieve a simultaneous, live imaging of single, label-free colloidal particle endocytosis by individual cells. The TIRM arm of the microscope enables label free imaging of the colloid and cell membrane features, while the TIRF arm images the dynamics of fluorescent-labeled clathrin (protein involved in endocytosis via clathrin pathway), expressed in transfected 3T3 fibroblasts cells. Using a model polymeric colloid and cells with a fluorescently tagged clathrin endocytosis pathway, we demonstrate that wide field TIRM/TIRF coimaging enables live visualization of the process of colloidal particle interaction with the labeled cell structure, which is valuable for discerning the membrane events and route of colloid internalization by the cell. We further show that 500 nm in diameter model polystyrene colloid associates with clathrin, prior to and during its cellular internalization. This association is not apparent with larger, 1 μ m in diameter colloids, indicating an upper particle size limit for clathrin-mediated endocytosis.

KEYWORDS: *imaging systems, total internal reflection fluorescence, live cell imaging, clathrin, endocytosis, evanescent wave microscopy*



INTRODUCTION

Interactions of a colloidal-size particle with the cellular membrane and the mechanisms of its cellular internalization and trafficking determine the resultant intracellular distribution of the particle and consequent effects on the cell. This applies to different colloidal particles including those designed for drug delivery purposes, such as polymer-based nanoparticles,¹ dendrimers,² polymer-drug conjugates,³ microparticles,⁴ and liposomes,⁵ or different nanomaterials, such as iron-oxide contrast agents or quantum dots.⁶

Some of the first attempts to visualize the subcellular structures involved in endocytosis of colloidal particles, such as clathrin coated pits (CCPs), were performed using transmission electron microscopy (TEM).⁷ Despite achieving unparalleled resolution, electron microscopy methods provide a static snapshot on fixed cell specimens,⁸ rather than real-time live imaging that would afford deeper understanding on the endocytosis process and pathways involved. Substantial progress is evident in high-resolution imaging of the endocytic machinery involved in the internalization of colloidal particles by living cells, utilizing a number of microscopy techniques including: (i) optical techniques, such as differential interference contrast (DIC) or confocal laser scanning microscopy (CLSM),^{9–14} and (ii) scanning probe techniques, such as

atomic force microscopy (AFM),^{15,16} near-field scanning optical microscopy (NSOM),¹⁷ scanning surface confocal microscopy (SSCM),¹⁸ and scanning ion-conductance microscopy (SICM).¹⁹

Currently, the most widely used imaging techniques, such as confocal laser microscopy, allow live imaging of biological specimens, but they require the use of a fluorescent label to mark both cellular structure(s) implicated in the process, as well as the colloidal particle of interest.^{12,20–22} Stable fluorescent labeling of colloidal particles requires development of an appropriate labeling protocol,²³ determined in each case by the chemistry of the colloid, meaning a bespoke procedure is needed for each system. Furthermore, development of a labeling procedure is not practical for screening a number of different nanomaterials/colloids, for instance, in cell internalization and toxicity studies. The introduction of a fluorescent label to the colloidal particle may also give rise to additional issues of photobleaching and phototoxicity to the cell, making long-term studies less practical.²⁴ Evidently, there is a need to

Received: March 17, 2015

Revised: September 22, 2015

Accepted: September 24, 2015

Published: September 24, 2015

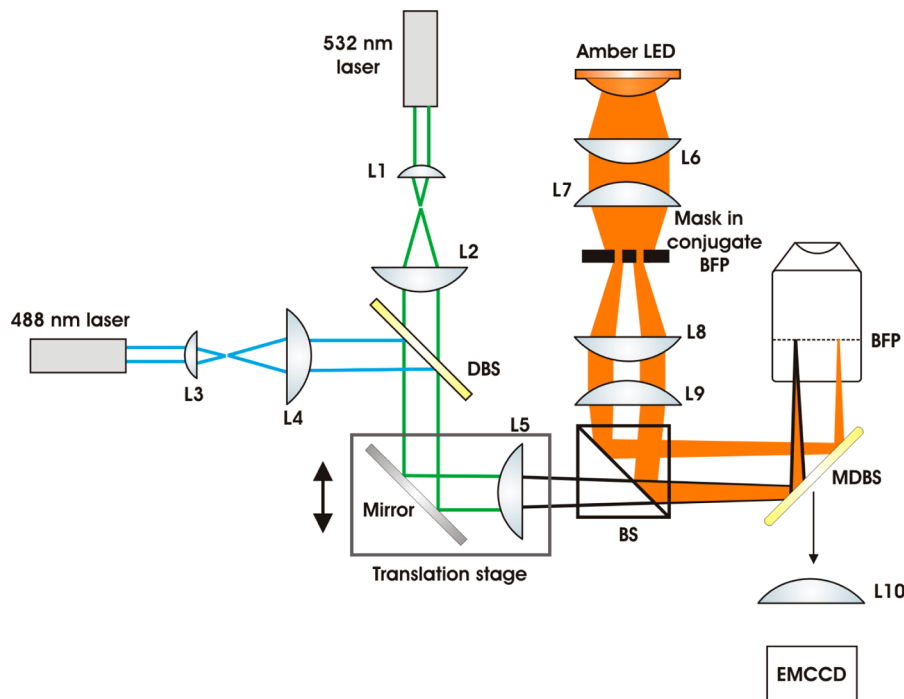


Figure 1. Schematic representation of the experimental setup configuration. For the two color TIRF illumination, the laser beams are expanded by lenses L1–4 and combined at a dichroic beam splitter (DBS). To control the incident illumination angle, the mirror and focusing lens L5 can be translated by the stage to allow positioning of the focal point in the back focal plane (BFP) of the microscope objective lens. For TIRM illumination, the amber LED is imaged by condenser lenses L6 and L7 onto an annular mask that is conjugate to the BFP of the microscope objective. Lenses L8 and L9 image the mask into the BFP to provide illumination above the critical angle. Fluorescent emission and reflected LED illumination pass through the multiband dichroic beamsplitter (MDBS), and tube lens L10 forms an image on the electron multiplying charge-coupled device (EMCCD).

develop high-resolution live cell imaging techniques to study nanoparticle–cell or cell–substrate interactions but without the need to fluorescently label the colloid/substrate and/or the cell.

Recently, to address the above issues we introduced a total internal reflection microscope (TIRM) capable of *in situ* label-free imaging of colloidal particle internalization by living cells.²⁵ The penetration depth (decay) of the evanescent field varies with incident angle, ranging from approximately 180 nm when the incident beam is 2 degrees above the critical angle to about 120 nm when the incident beam angle is increased by a further 5 degrees. Similar was previously reported for variable TIRF microscopy.²⁶ This means that both the TIRM and TIRF imaging fields are localized at the plasma membrane of a cell in contact with the substrate. The lateral resolution of both TIRM and TIRF imaging channels is diffraction limited at close to 200 nm.

We suggest that TIRM would be a “natural partner” for TIRF because both imaging techniques have comparable lateral resolution, axial localization, and field of view (as depicted in Figure 1) as opposed to, for example, TIRF in combination with differential interference contrast (DIC) as another label-free imaging technique. The latter is a powerful combination, but the temporal and spatial resolution of DIC was shown to be limited when used in combination with TIRF.²⁷ TIRM/TIRF is therefore a potentially useful tool in the study of cellular membrane events, such as with colloidal particle interaction, with improved spatial resolution, especially in the axial direction.

In the present work we describe the application of combined TIRM/TIRF microscopy to cloned cells expressing GFP-clathrin to visualize label-free colloidal particles close to the

membrane and study their internalization in a living cell. In our experimental set up, the colloid and cell membrane are unlabeled and imaged by the TIRM arm of the microscope, while the endocytic structure of interest, clathrin, is expressed in genetically modified cells conjugated with green fluorescent protein (GFP), which is visualized by TIRF. We demonstrate that the TIRM/TIRF microscope can be used to distinguish the uptake pathways of 500 nm model polymeric colloids in 3T3 fibroblast cells. Indeed, we achieved a direct visualization of the formation of clathrin coated pits (CCP) around the colloidal particle, prior to internalization by the cell.

MATERIALS AND METHODS

Cell Culture. Murine fibroblast (3T3) cells were obtained from the European Collection of Cell Cultures (ECACC). The cells were cultured in Dulbecco’s Modified Eagle’s Medium (DMEM), supplemented with 10% new born calf serum (NBCS), 1 unit/mL penicillin, 1 mg/mL streptomycin, 2.5 µg/mL amphotericin B (antibiotic/antimycotic solution), and 1% L-glutamine, in a humidified incubator at 37 °C and 5% CO₂. Every 6–7 days the cells were removed from the tissue culture flasks, using 0.25% trypsin and 1 mM ethylenediaminetetraacetic acid (EDTA) in phosphate buffered saline (PBS), and reseeded.

Plasmid Construction. mRNA extraction and cDNA synthesis from murine 3T3 cell extracts was accomplished using a μMACS One-Step cDNA kit (Miltenyi Biotec). Full-length mouse clathrin light chain (mLCA) was amplified from the cDNA using the PfxUltima PCR system (Invitrogen, UK) and the following primers: forward 5' GCCCGGGGAATTC-CATGGCCGAGTTGGATCCAT (EcoRI site underlined),

reverse 5' GCCCGGGTACCTCAGTGCACCAGGGGGGCC (*Kpn*I site underlined). The resulting PCR product was cloned directly into pEGFP-C1 (Clontech, BD Bioscience, Palo Alto, CA) using the *Eco*RI and *Kpn*I sites to produce mLCA-EGFP (clathrin–EGFP).

Transfection of Cells. Stocks of 3T3 cells were maintained in 6-well plates (Corning Life Sciences, France) at 5% CO₂ in DMEM (Sigma-Aldrich, UK) supplemented with 10% fetal calf serum (FCS). For transfection, cells were grown to 80% confluence and transfected with 5 µg plasmid DNA using TransFast Transfection Reagent (Promega, UK) in accordance with the manufacturer's instructions.

Preparation Deposition for TIRM/TIRF Uptake Studies. Glass based dishes (35 mm, Iwaki, Japan) were coated with a 0.01% poly L-lysine (PLL) solution (MW 70,000–150,000, Sigma-Aldrich, UK) for 15 min at room temperature. Following coating with PLL the dishes were rinsed three times with distilled water and once with PBS. Particle adhesion to the PLL coated surface was achieved by adding 1 mL of a 0.016% w/v suspension of surfactant-free white carboxyl latex (Interfacial Dynamics Corporation, Eugene, OR) to the dish for 30 min. The remaining suspension was subsequently removed, and the dish was rinsed with PBS.

Scanning Electron Microscopy (SEM). For SEM, samples were fixed in 3% glutaraldehyde in 0.1 M sodium cacodylate buffer, pH 7.3, for 2–3 h. The samples were then washed in 3 × 10 min changes of 0.1 M sodium cacodylate buffer. Specimens were then postfixed in 1% osmium tetroxide in 0.1 M sodium cacodylate buffer for 45 min, prior to being washed in three 10 min changes of 0.1 M sodium cacodylate buffer. The samples were then dehydrated in 50%, 70%, 90%, and 100% normal grade acetone for 10 min each, then for a further two 10 min changes in analar acetone. Dehydrated samples were then critical point dried, mounted on aluminum stubs, and sputter coated with gold palladium.

TIRM/TIRF Microscopy. A combination of TIRM and TIRF utilizing illumination through the microscope objective (PlanFluor 100× NA 1.45, Zeiss) was performed using a standard inverted biological microscope (TC 5400, Meiji) with custom-built illumination optics. The optical configuration used for TIRF imaging of clathrin-EGFP included excitation with a 488 nm solid state laser (Protera 488-15, Novalux, Sunnyvale, CA) reflected off a polychroic mirror (z488/532). Emitted light was collected through a suitable emission filter (z488/532m). All filters and polychroic and dichroic mirrors were obtained from Chroma Technologies (Brattleboro, VT). TIRM imaging of 3T3 cells was achieved with illumination using a light emitting diode (LED) with a center wavelength of 580 nm (LXHL-ML1D Luxeon Star, Lumileds, CA) reflected off the same polychroic mirror. This wavelength was chosen to ensure the fluorophores were not excited by the TIRM channel. In order to minimize the chromatic aberration, as short a wavelength as possible was chosen compatible with nonexciting fluorescence. After total internal reflection from the sample the illumination light is transmitted through both the polychroic mirror and emission filter with 85% efficiency, resulting in approximately 11% of the initial illumination reaching the camera, which was sufficient to provide bright TIRM images; while giving >80% transmission of the fluorescent wavelengths through the polychroic mirror and the emission filter.

The camera utilized to acquire images was a 14-bit cooled EMCCD (iXon DV-885 KCS-VP, Andor Technology, Belfast UK). The resolution of the camera was 1004 × 1002 pixels,

with each pixel 8 µm × 8 µm in size. Sequential TIRM and TIRF images were acquired by the camera under the control of iQ version 1.5 (Andor Technologies, Belfast UK). Mechanical shutters, also under the control of iQ via a breakout box (Andor Technologies, Belfast UK), were placed in the beam path to minimize photobleaching and to switch between TIRM and TIRF illumination. TIRM and TIRF images were acquired with exposure times of 90 and 400 ms, respectively.

Image Analysis. For overlaying of TIRM and TIRF video sequences, they were first streamed to a kinetic image disc on a PC (Dell, UK). The images from each channel (TIRM and TIRF) were then imported into ImageJ as an image sequence. Sixteen-bit images were converted to RGB images. The RGB images were false colored using the look-up table (LUT) function on ImageJ. TIRF images were pseudocolored green for EGFP-clathrin, and TIRM images underwent an inverse LUT prior to a red LUT being applied. The image sequences were overlaid using the image calculator function in ImageJ and summer where appropriate. The resulting combination image was finally cropped and saved as an Avi file.

RESULTS AND DISCUSSION

The experimental setup adopted in the present study to perform TIRM/TIRF imaging of cell internalization events occurring at the membrane is illustrated in Figure 1. The classical experimental model to study cellular endocytosis of colloidal particles involves the addition of a colloid suspension to cells grown on a culture substrate, followed by quantitation of uptake using fluorescence microscopy, flow cytometry, or spectroscopy on digested cells.⁹ This model is relatively simple to arrange and has been performed in numerous studies, e.g., refs 9, 12, and 28–30. To allow the use of TIRM/TIRF imaging, with the imaging depth in the order of 200 nm in the axial direction from the adherent cell membrane, the colloidal particles were adhered to the surface of a polylysine (PLL) treated coverslip (PLL treatment being a standard cell culture protocol to promote attachment)³¹ to which the cells (suspended in culture medium) were subsequently added.

The scanning electron microscopy image in Figure 2A shows a cell and polystyrene colloidal particle (2.0 µm) at 30 min time point following addition of a cell suspension to substrate adhered colloid. At this stage the cell still possesses spherical morphology, likely due to the relatively short length of time it was exposed to the treated substrate surface, with protrusions of the cell membrane (lamellipodial and filopodia) present. Figure 2B shows cell morphology 60 min later in the incubation period, illustrating an advanced stage of the cell-colloidal particle interaction/internalization process. The image illustrates that the cell membrane is beginning to veil over the two particles adhered to the treated surface, suggesting the initial stages of cellular internalization. These SEM images demonstrate that the experimental setup (as illustrated in Figure 1) used for the TIRM/TIRF microscopy is suitable for the study of cell–colloid interactions.

It should be noted that our experimental set up shares its main arrangement properties with some other reported studies, particularly “substrate mediated delivery” approaches,^{32–37} where delivery colloids are immobilized to a surface, or a biomaterial, that supports cell adhesion. Polystyrene colloids of 2 µm in diameter were chosen for the purposes of SEM imaging (Figure 2) to aid their visualization and distinction from cellular structures. Previously, we have demonstrated that these particles are internalized by 3T3 cells.²⁵

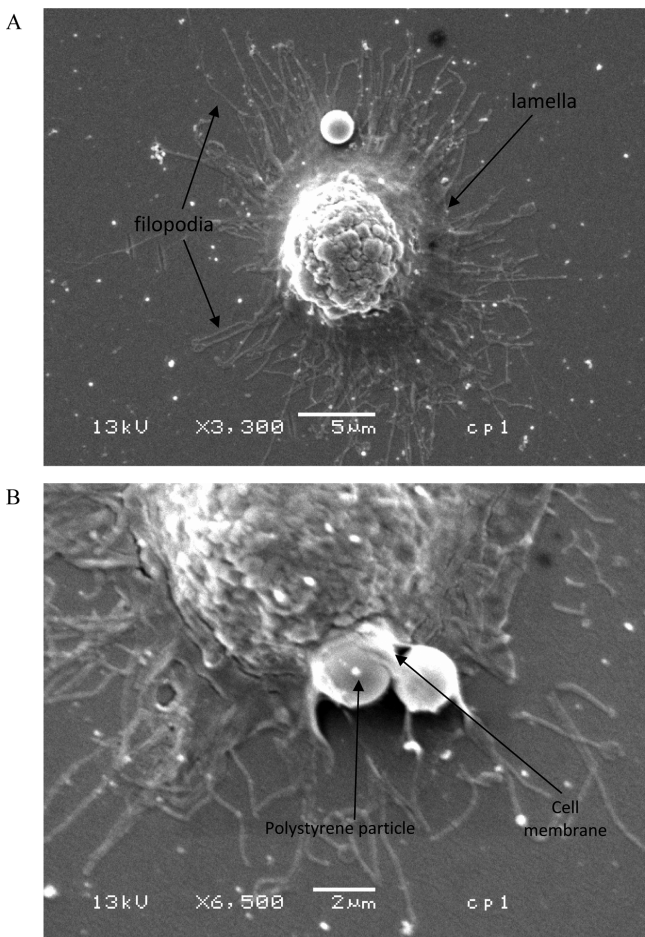


Figure 2. SEM images of 2 μm in diameter polystyrene colloid and a 3T3 fibroblast cell. (A) Membrane and filopodia of a 3T3 cell 30 min following addition of cells to surface adhered colloid. (B) A 3T3 cell with colloidal particles at 60 min time point showing that the membrane is beginning to engulf the colloidal particles.

In our previous work, which focused on the design of the TIRM/TIRM microscope, we demonstrated that a TIRM arm of the current instrument is *per se* capable of imaging individual cells and their internalization of label-free submicron colloid;

further confirmed by confocal microscopy using fluorescently labeled colloid and conventional cell tracker orange-labeling of the cells.²⁵ However, TIRM imaging on its own could not access information on the membrane constituent(s) involved in the cell–colloid interaction and consequently identify which internalization pathway was involved. The present study focuses on the potential of combined TIRM/TIRF microscopy to visualize the events occurring at cellular membrane during endocytosis of a colloidal particle *in situ* and to, simultaneously, identify the pathway involved in colloid internalization. To this end, the EGFP-clathrin LCa fusion protein was successfully developed and expressed in murine 3T3 fibroblast cells. A plasmid encoding enhanced GFP was attached to the N-terminus of mouse placental clathrin “light chain a” (LCa) and the protein expressed. Previously, it has been shown that this type of EGFP-clathrin LCa conjugate is incorporated into structurally and functionally active clathrin trimers and coated pits in cells, and that cells expressing GFP–clathrin were active in receptor-mediated endocytosis.³⁸ Indeed, this construct has been used successfully by several authors to study the clathrin mediated endocytosis pathway.^{39–41}

Figure 3 illustrates the use of TIRM/TIRF combination microscopy. Image A represents TIRF of an individual 3T3 fibroblast cell whereby discrete green puncta are understood to correspond to cellular membrane structures formed by association of EGFP-clathrin molecules (coated pits) and clathrin coated vesicles (clathrin coated pits that are progressively invaginating, undergone scission, and are being released into the cell cytosol), which are present intracellularly at/or in proximity of the adherent membrane within the imaging depth of TIRF of less than 200 nm. For a clearer visualization of discrete fluorescent puncta, a low-spatial frequency background due to cytoplasmic EGFP-clathrin has been removed from the image. This was achieved by low pass filtering to remove background and low spatial frequencies, gaining images free from fluorescence due to cytoplasmic clathrin. TIRM in image B shows the cellular membrane and structures in the membrane proximity within the TIRM imaging depth of the same fibroblast cell. The mechanism for the image formation of the label-free images is discussed in some detail previously.²⁵ In essence, we may consider the mechanism to be akin to frustrated total internal reflection. For a uniform object with relative low refractive index, total internal

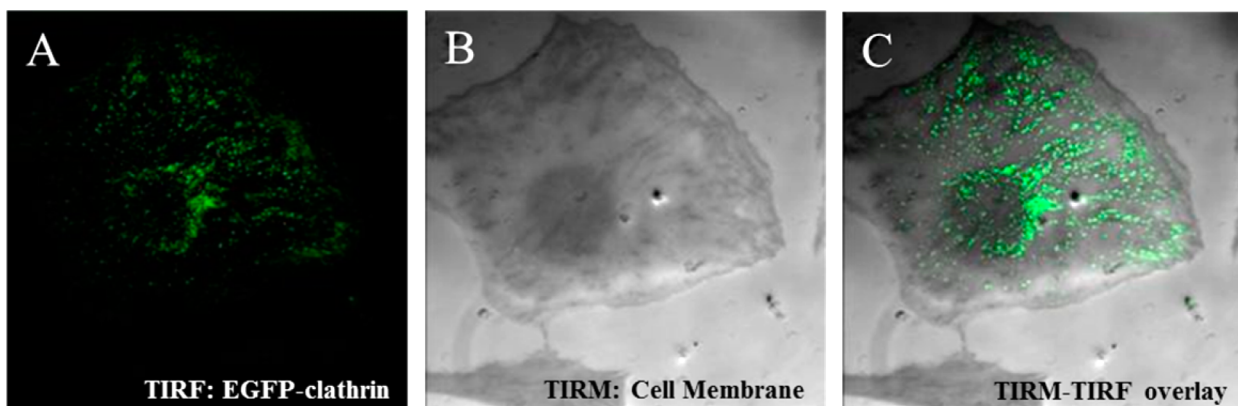


Figure 3. TIRM/TIRF analysis of clathrin distribution in a 3T3 fibroblast cell 24 h post-transfection. (A) TIRF image of a 3T3 fibroblast cell transfected with EGFP-clathrin. For a clearer visualization of discrete fluorescent spots, a low-spatial frequency background due to cytoplasmic EGFP-clathrin has been subtracted from the image. (B) TIRM image of the same fibroblast cell captured immediately following the TIRF image. (C) Combined TIRM/TIRF image highlighting the distribution of clathrin puncta on the cell membrane.

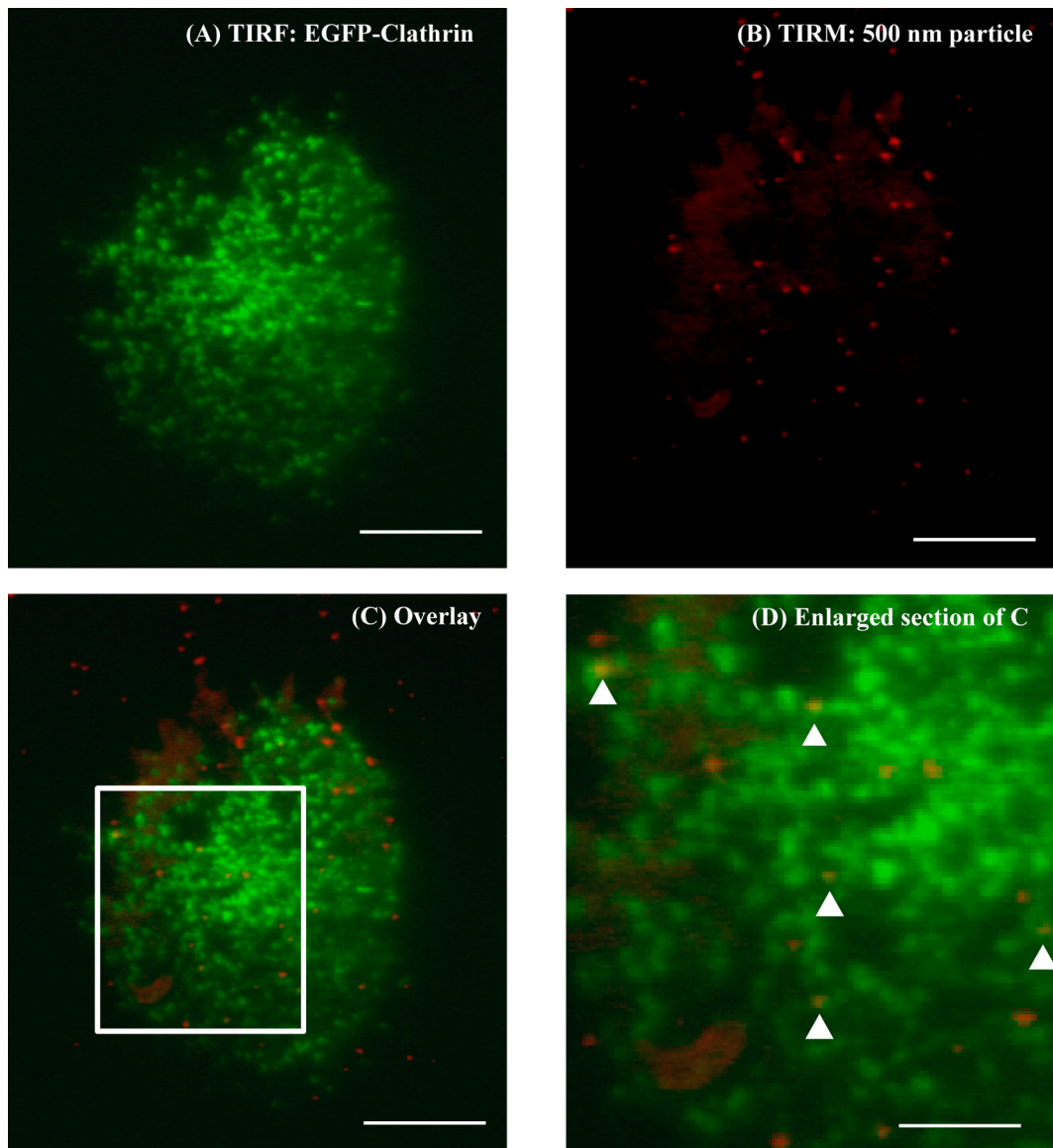


Figure 4. Low magnification TIRM/TIRF imaging of 500 nm (diameter) polystyrene colloid undergoing endocytosis by EGFP-clathrin Lca transfected 3T3 cells. (A) TIRF image of EGFP-clathrin Lca. (B) Label-free TIRM image of 500 nm carboxyl modified polystyrene particle adhered to the surface of a polylysine coated substrate. A red false color look-up table (LUT) was applied to aid colocalization studies. (C) Overlay of the TIRF and TIRM images. (D) Magnified section of the TIRM/TIRF overlay of image in C, as represented by the white outline. Yellow puncta (highlighted by the white triangles) represent the colocalization of EGFP-clathrin and the 500 nm colloid. Scale bar represents 15 μm (panels A–C) and 6 μm (panel D).

reflection will occur and the image will appear bright and homogeneous since all the light is evenly reflected. When an object moves into the evanescent field, which either scatters or refracts light into propagating light, energy is removed from the incident beam resulting in a reduced intensity of the internally reflected light. The label free mode is thus sensitive to the presence of objects (such as cell membrane), which impinge the evanescent field. In general, the image will appear darker as the cell membrane approaches the surface of the substrate (coverslip).

Figure 3C, an overlay of images A and B, illustrates how combined TIRM/TIRF microscopy can be applied to study an event occurring at the nonlabeled cell membrane in contact with the substrate (e.g., membrane ruffling) by nonfluorescent TIRM at very high resolution of topographical information (relative to “standard brightfield” light microscopy), while

concurrently viewing fluorescently labeled cellular structures of interest. This image highlights the advantages associated with TIRM/TIRF imaging of biological samples; low background fluorescence, high signal-to-noise, and high image contrast. It should be also noted that, unlike a brightfield image, TIRM allows well-localized imaging of events at, or close to, the adherent cell membrane.

The direction of migration of the cell in Figure 3 (approximately from lower left toward upper right corner of the image) and corresponding distribution of EGFP-clathrin signal, sparsely distributed at the “lagging side” of the cell and progressively denser toward the “leading edge”, is similar to that previously described for Madine Darby Canine Kidney (MDCK) cells.⁴² The denser spatial positioning of clathrin toward the leading edge of the cell was attributed to the processes of exocytosis and endocytosis functioning to adjust

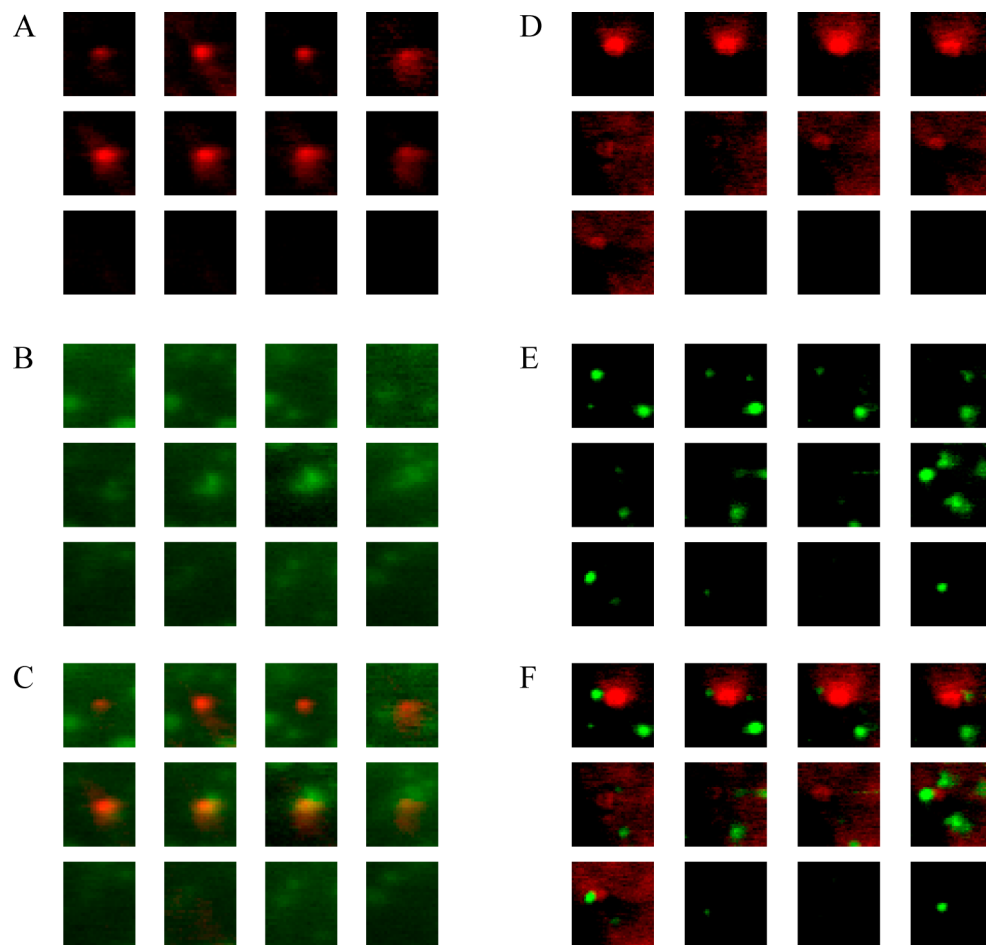


Figure 5. TIRM/TIRF images of polystyrene colloid endocytosis by 3T3 cells expressing EGFP-Clathrin LCa. Cellular uptake of 500 nm (A–C panels) and 1.0 μm (diameter) polystyrene colloids (D–F panels), shown in 12 sequential frames selected from a sequence of 100 at 2 min per frame. (A) Twelve sequential TIRM images of a 500 nm particle. The particle is internalized over the time-course of 12 sequential frames (i.e., 24 min in total). Images have been pseudocolored red and inverted to aid colocalization analysis. (B) Twelve sequential TIRF images of EGFP-Clathrin LCa. Clathrin is observed to increase in intensity between frames 5–7, i.e., over a period of 6 min. Images are pseudocolored green. (C) Overlay of TIRM and TIRF images in A and B. Frames 5–8 show colocalization of clathrin and 500 nm particle. (D) Twelve sequential TIRM images of a 1 μm particle. The particle is internalized over the time-course of the presented frames (24 min in total). (E) Twelve sequential TIRF images of EGFP-Clathrin LCa. The image sequence depicts movement of clathrin puncta. (F) Overlay of TIRM and TIRF images in C and D. Although clathrin can be seen to be in close proximity to the particle, there is no colocalization like that seen with the 500 nm particle. Panels A, B, and C are equivalent to 2.5 μm ; panels D, E, and F are equivalent to 4 μm .

membrane tension to facilitate the generation of motile force or internalization of chemokines, cytokines, and growth factors.⁴² It must be noted that preferential distribution at the leading edge of fibroblasts cells also applies to clathrin-independent carriers, with this polarization playing a critical role during cell migration.⁴³

Figure 4A is an image of a 3T3 cell expressing EGFP-clathrin taken using the TIRF channel of the TIRM/TIRF microscope. In panel B, TIRM was used to image 500 nm diameter colloids adhered to a PLL-coated coverslip (colloid false-colored red to aid colocalization analysis when TIRM and TIRF images are overlaid). Overlaid TIRM and TIRF images are presented in panel C and a magnified section of this image is shown in panel D. The colocalization of clathrin with the 500 nm colloid is represented by the presence of yellow puncta in the overlaid image (marked by the arrowhead). Image analysis reveals that there were a total of 35 colloidal particles adhered to the PLL-coated surface, which is presented to the adherent cell membrane. Of these, 13 particles (37%) are colocalized with EGFP-clathrin.

Panel A in Figure 5 shows a series of 12 images (captured at intervals of 2 min per image frame) from a typical TIRM time-lapse sequence, which depicts (from top left to bottom right image) the presence of the colloidal particle in images 1 to 8, followed by its disappearance between images 8 and 9. TIRF images in panel B show the EGFP-clathrin signal captured 100 ms prior to the TIRM image at the exact spatial location of the specimen cell. Following the images (from top left to bottom right) a gradual increase in the EGFP-clathrin intensity is evident in images 1 to 8, followed by loss in the fluorescent signal between images 8 and 9, i.e., within 2 min. Panel C (Figure 5) is the resultant TIRM/TIRF overlay. An increase in yellow color intensity between images 5 and 8 indicates the colocalization of the EGFP-clathrin (TIRF, green) with the 500 nm colloid (TIRM, red). The disappearance of all signals (red TIRM, green TIRF, and yellow overlap) after image 8 indicates that the 500 nm colloid has been internalized by the cell, i.e., both the particle and clathrin have moved outside the microscope's axial imaging range of approximately 200 nm.

Panels D–F in **Figure 5** show the results for an experiment identical to that described above, except that the 500 nm colloid was replaced by 1.0 μm counterpart. Panel D shows the disappearance of a 1.0 μm particle between image frames 4 and 5. The EGFP-clathrin signal captured 100 ms prior to the TIRM image, at the same spatial location of the specimen cell is shown in panel E. Panel F (overlay) demonstrates that there is no colocalization of EGFP-clathrin with the 1.0 μm colloid during the particle internalization event (between frames 4 and 5).

The correlation of the TIRF EGFP-clathrin with the TIRM colloid imaging suggests that the 500 nm-sized (diameter) particle was internalized by cells via a clathrin-mediated pathway. The time between each image/frame shown in panels of **Figure 5** is 2 min, which thus indicates that from the initial association of clathrin (panel B, image frame 5) with the particle at the adherent cell membrane, it takes approximately 6 min prior to the internalization event (panel B, image frame 8). This period of clathrin persistence represents the time needed for the cell to recruit enough clathrin to the site to form a clathrin-coated pit and thus enable internalization of the material. The increasing EGFP-clathrin signal in images shown in **Figure 5** (panel B) represents this process of recruitment of clathrin to the endocytic site. Following the recruitment of clathrin to form a clathrin coated pit, it is likely that this leads to the formation of a clathrin coated vesicle (detached from the cell membrane), as suggested by the rapid disappearance of both the TIRM (particle) and TIRF (clathrin) signal from the evanescent field.

Literature reports on studies of a single colloidal particle endocytosis by a single cell, where the mechanism of internalization has been elucidated, to allow a comparison of our data, are rare. However, from the literature it is evident that the lifetimes of clathrin puncta at the membrane are variable, ranging from seconds to several minutes.^{44–46} Lifetimes in the order of minutes, as we show here, have been reported before. A study using combined TIR and WF fluorescence microscopy to examine formation of clathrin structures tagged with LCa-DsRed showed structures that have a constant fluorescence signal and are relatively long-lived (>200 s) at the adherent surface of Swiss 3T3 cells.^{47,48} Other authors have also reported similar findings,^{49–52} including a study that used a TIR-WF protocol and describes long-lived endocytic clathrin structures, naming them “clathrin-coated plaques”.⁵³

The involvement of clathrin-mediated uptake in cellular uptake of 500 nm diameter particles seen here would be above “size limit” reported previously in murine melanoma cell line B16, as assessed by employing pharmacological inhibitors to determine endocytic route (versus direct visualization in the present study). The study concluded that caveolae-mediated internalization is a predominant pathway of entry for 500 nm particles.⁹ In contrast, clathrin-dependent uptake of larger cargoes was demonstrated in studies showing clathrin participation in the cellular entry of *L. monocytogenes*, other bacteria, and large viruses using a so-called “zipper mechanism”.^{44,54–56}

Regarding internalization of 1 μm diameter colloid by a nonclathrin-dependent process by 3T3 cells observed here, particles of this size were not internalized by B12 cells in the above study,⁹ although a recent paradigm shift on the role of clathrin in internalization of large cargos (particularly pathogenic bacteria and large viruses) suggests that clathrin-mediated endocytosis machinery may be acting in a form of

“planar clathrin lattices” of membrane domains; however, this is still poorly characterized.⁵⁷ Our study indicates that in 3T3 cells internalization of 1 μm polystyrene colloid can occur, although the process does not appear to be mediated by clathrin machinery.

CONCLUSIONS

In summary, we have developed a novel experimental tool to directly visualize the initial stages of single colloidal particle internalization in a living cell. This methodology is particularly powerful as it does not require either the colloidal particle system (e.g., drug delivery carrier) or the cell structures to be labeled to enable live visualization. Furthermore, we illustrate that through the use of cloned cells expressing specifically fluorescently tagged endocytic proteins, this technology enables elucidation of the endocytic pathway for particular colloid systems by combined TIRF/TIRM. We demonstrate the application of TIRM/TIRF technology developed by showing the colocalization of GFP-clathrin with 500 nm colloidal particles and their subsequent internalization into the cell, indicating a clathrin mediated route of endocytosis. We also show a lack of such colocalization for larger 1 μm colloid, suggesting that the cellular internalization in this case does not occur via the clathrin pathway.

AUTHOR INFORMATION

Corresponding Author

*E-mail: snow.stolnik@nottingham.ac.uk. Tel: +44(0)115 8466074. Fax: +44(0)115 9515102.

Present Addresses

[†]Merck Sharp & Dohme, DevLab, Hoddesdon, EN11 9BU, U.K.

[‡]School of Pharmacy, University of Lincoln, Joseph Banks Laboratories, Green Lane, Lincoln, LN6 7DL, U.K.

[#]Department of Electronic and Information Engineering, Hong Kong Polytechnic University, Hung Hom, Kowloon, Hong Kong.

Notes

The authors declare no competing financial interest.

ACKNOWLEDGMENTS

We are grateful to the University of Nottingham Interdisciplinary Doctoral Training Centre in Nanoscience and Nanotechnology for funding.

ABBREVIATIONS

TIRF, total internal reflection fluorescence; TIRM, total internal reflection microscopy

REFERENCES

- (1) Na, K.; Seong Lee, E.; Bae, Y. H. Adriamycin loaded pullulan acetate/sulfonamide conjugate nanoparticles responding to tumor pH: pH-dependent cell interaction, internalization and cytotoxicity in vitro. *J. Controlled Release* **2003**, *87* (1–3), 3–13.
- (2) Hong, S.; Bielinska, A. U.; Mecke, A.; Keszler, B.; Beals, J. L.; Shi, X.; Balogh, L.; Orr, B. G.; Baker, J. R.; Banaszak Holl, M. M. Interaction of Poly(amidoamine) dendrimers with supported lipid bilayers and cells: Hole formation and the relation to transport. *Bioconjugate Chem.* **2004**, *15* (4), 774–782.
- (3) Luo, Y.; Bernshaw, N. J.; Lu, Z. R.; Kopecek, J.; Prestwich, G. D. Targeted delivery of doxorubicin by HPMA copolymer-hyaluronan bioconjugates. *Pharm. Res.* **2002**, *19* (4), 396–402.

- (4) Coombes, A. G. A.; Tasker, S.; Lindblad, M.; Holmgren, J.; Hoste, K.; Toncheva, V.; Schacht, E.; Davies, M. C.; Illum, L.; Davis, S. S. Biodegradable polymeric microparticles for drug delivery and vaccine formulation: the surface attachment of hydrophilic species using the concept of poly(ethylene glycol) anchoring segments. *Biomaterials* **1997**, *18* (17), 1153–1161.
- (5) Miller, C. R.; Bondurant, B.; McLean, S. D.; McGovern, K. A.; O'Brien, D. F. Liposome-Cell Interactions in Vitro: Effect of Liposome Surface Charge on the Binding and Endocytosis of Conventional and Sterically Stabilized Liposomes. *Biochemistry* **1998**, *37* (37), 12875–12883.
- (6) Osaki, F.; Kanamori, T.; Sando, S.; Sera, T.; Aoyama, Y. A quantum dot conjugated sugar ball and its cellular uptake. On the size effects of endocytosis in the subviral region. *J. Am. Chem. Soc.* **2004**, *126*, 6520–6521.
- (7) Heuser, J. Three-dimensional visualization of coated vesicle formation in fibroblasts. *J. Cell Biol.* **1980**, *84* (3), 560–583.
- (8) Torgersen, M. L.; Skretting, G.; van Deurs, B.; Sandvig, K. Internalization of cholera toxin by different endocytic mechanisms. *Journal of Cell Science* **2001**, *114* (20), 3737–3747.
- (9) Rejman, J.; Oberle, V.; Zuhorn, I. S.; Hoekstra, D. Size-dependent internalization of particles via the pathways of clathrin- and caveolae-mediated endocytosis. *Biochem. J.* **2004**, *377* (1), 159–169.
- (10) Zhang, Y.; Kohler, N.; Zhang, M. Surface modification of superparamagnetic magnetite nanoparticles and their intracellular uptake. *Biomaterials* **2002**, *23* (7), 1553–1561.
- (11) Rosi, N. L.; Giljohann, D. A.; Thaxton, C. S.; Lytton-Jean, A. K. R.; Han, M. S.; Mirkin, C. A. Oligonucleotide-Modified Gold Nanoparticles for Intracellular Gene Regulation. *Science* **2006**, *312* (5776), 1027–1030.
- (12) Panyam, J.; Labhasetwar, V. Dynamics of Endocytosis and Exocytosis of Poly (D, L-Lactide-co-Glycolide) Nanoparticles in Vascular Smooth Muscle Cells. *Pharm. Res.* **2003**, *20* (2), 212–220.
- (13) Desai, M. P.; Labhasetwar, V.; Walter, E.; Levy, R. J.; Amidon, G. L. The Mechanism of Uptake of Biodegradable Microparticles in Caco-2 Cells Is Size Dependent. *Pharm. Res.* **1997**, *14* (11), 1568–1573.
- (14) Sandin, P.; Fitzpatrick, L. W.; Simpson, J. C.; Dawson, K. A. High-Speed Imaging of Rab Family Small GTPases Reveals Rare Events in Nanoparticle Trafficking in Living Cells. *ACS Nano* **2012**, *6* (2), 1513–1521.
- (15) Shukla, R.; Bansal, V.; Chaudhary, M.; Basu, A.; Bhonde, R. R.; Sastry, M. Biocompatibility of Gold Nanoparticles and Their Endocytotic Fate Inside the Cellular Compartment: A Microscopic Overview. *Langmuir* **2005**, *21* (23), 10644–10654.
- (16) Vasir, J. K.; Labhasetwar, V. Quantification of the force of nanoparticle-cell membrane interactions and its influence on intracellular trafficking of nanoparticles. *Biomaterials* **2008**, *29* (31), 4244–4252.
- (17) Yu, Z.; Yazdanpanah, V.; Mo, Y.; Ozkan, M.; Ozkan, C. S. In *Normal and Cancer Breast Epithelial Cells Endocytosis Study of Nanoparticles by Combined AFM and NSOM Microscopy*; 7th IEEE Conference, 2007; pp 1028–1032.
- (18) Gorelik, J.; Shevchuk, A.; Ramalho, M.; Elliott, M.; Lei, C.; Higgins, C. F.; Lab, M. J.; Klenerman, D.; Krauzewicz, N.; Korchev, Y. Scanning surface confocal microscopy for simultaneous topographical and fluorescence imaging: Application to single virus-like particle entry into a cell. *Proc. Natl. Acad. Sci. U. S. A.* **2002**, *99* (25), 16018–16023.
- (19) Novak, P.; Shevchuk, A.; Ruenraroengsak, P.; Miragoli, M.; Thorley, A. J.; Klenerman, D.; Lab, M. J.; Tetley, T. D.; Gorelik, J.; Korchev, Y. E. Imaging single nanoparticle interactions with human lung cells using fast ion conductance microscopy. *Nano Lett.* **2014**, *14* (3), 1202–1207.
- (20) Jiang, X.; Röcker, C.; Hafner, M.; Brandholt, S.; Dörlich, R. M.; Nienhaus, G. U. Endo- and Exocytosis of Zwitterionic Quantum Dot Nanoparticles by Live HeLa Cells. *ACS Nano* **2010**, *4* (11), 6787–6797.
- (21) Clift, M. J. D.; Rothen-Rutishauser, B.; Brown, D. M.; Duffin, R.; Donaldson, K.; Proudfoot, L.; Guy, K.; Stone, V. The impact of different nanoparticle surface chemistry and size on uptake and toxicity in a murine macrophage cell line. *Toxicol. Appl. Pharmacol.* **2008**, *232* (3), 418–427.
- (22) dos Santos, T.; Varela, J.; Lynch, I.; Salvati, A.; Dawson, K. A. Quantitative Assessment of the Comparative Nanoparticle-Uptake Efficiency of a Range of Cell Lines. *Small* **2011**, *7* (23), 3341–3349.
- (23) Qaddoumi, M. G.; Gukasyan, H. J.; Davda, J.; Labhasetwar, V.; Kim, K. J.; Lee, V. H. Clathrin and caveolin-1 expression in primary pigmented rabbit conjunctival epithelial cells: role in PLGA nanoparticle endocytosis. *Molecular Vision* **2003**, *9*, 559–568.
- (24) Song, C. X.; Labhasetwar, V.; Murphy, H.; Qu, X.; Humphrey, W. R.; Shebuski, R. J.; Levy, R. J. Formulation and characterization of biodegradable nanoparticles for intravascular local drug delivery. *J. Controlled Release* **1997**, *43* (2–3), 197–212.
- (25) Byrne, G. D.; Pitter, M. C.; Zhang, J.; Falcone, F. H.; Stolnik, S.; Somekh, M. G. Total internal reflection microscopy for live imaging of cellular uptake of sub-micron non-fluorescent particles. *J. Microsc.* **2008**, *231*, 168–179.
- (26) Stock, K.; Sailer, R.; Strauss, W. S. L.; Lyttek, M.; Steiner, R.; Schneckenburger, H. Variable-angle total internal reflection fluorescence microscopy (VA-TIRFM): realization and application of a compact illumination device. *J. Microsc.* **2003**, *211*, 19–29.
- (27) Giannone, G.; Dubin-Thaler, B. J.; Rossier, O.; Cai, Y.; Chaga, O.; Jiang, G.; Beaver, W.; Döbereiner, H.-G.; Freund, Y.; Borisy, G.; Sheetz, M. P. Lamellipodial Actin Mechanically Links Myosin Activity with Adhesion-Site Formation. *Cell* **2007**, *128* (3), 561–575.
- (28) Deshpande, M. C.; Davies, M. C.; Garnett, M. C.; Williams, P. M.; Armitage, D.; Bailey, L.; Vamvakaki, M.; Armes, S. P.; Stolnik, S. The effect of poly(ethylene glycol) molecular architecture on cellular interaction and uptake of DNA complexes. *J. Controlled Release* **2004**, *97* (1), 143–156.
- (29) Harush-Frenkel, O.; Debottin, N.; Benita, S.; Altschuler, Y. Targeting of nanoparticles to the clathrin-mediated endocytic pathway. *Biochem. Biophys. Res. Commun.* **2007**, *353* (1), 26–32.
- (30) Chavanpatil, M. D.; Khadair, A.; Panyam, J. Surfactant-polymer Nanoparticles: A Novel Platform for Sustained and Enhanced Cellular Delivery of Water-soluble Molecules. *Pharm. Res.* **2007**, *24* (4), 803–810.
- (31) Mazia, D.; Schatten, G.; Sale, W. Adhesion of cells to surfaces coated with polylysine. Applications to electron microscopy. *J. Cell Biol.* **1975**, *66* (1), 198–200.
- (32) Pannier, A. K.; Anderson, B. C.; Shea, L. D. Substrate-mediated delivery from self-assembled monolayers: Effect of surface ionization, hydrophilicity, and patterning. *Acta Biomater.* **2005**, *1* (5), 511–522.
- (33) Levy, R. J.; Song, C.; Tallapragada, S.; DeFelice, S.; Hinson, J. T.; Vyavahare, N.; Connolly, J.; Ryan, K.; Li, Q. Localized adenovirus gene delivery using antiviral IgG complexation. *Gene Ther.* **2001**, *8* (9), 659–667.
- (34) Segura, T.; Volk, M. J.; Shea, L. D. Substrate-mediated DNA delivery: role of the cationic polymer structure and extent of modification. *J. Controlled Release* **2003**, *93* (1), 69–84.
- (35) Segura, T.; Chung, P. H.; Shea, L. D. DNA delivery from hyaluronic acid-collagen hydrogels via a substrate-mediated approach. *Biomaterials* **2005**, *26* (13), 1575–1584.
- (36) Shen, H.; Tan, J.; Saltzman, W. M. Surface-mediated gene transfer from nanocomposites of controlled texture. *Nat. Mater.* **2004**, *3*, 569–574.
- (37) Luo, D.; Saltzman, W. M. Enhancement of transfection by physical concentration of DNA at the cell surface. *Nat. Biotechnol.* **2000**, *18*, 893–895.
- (38) Gaidarov, I.; Santini, F.; Warren, R. A.; Keen, J. H. Spatial control of coated-pit dynamics in living cells. *Nat. Cell Biol.* **1999**, *1* (1), 1–7.
- (39) Snyders, L.; Zwickl, H.; Blaas, D. Human Rhinovirus Type 2 Is Internalized by Clathrin-Mediated Endocytosis. *Journal of Virology* **2003**, *77* (9), 5360–5369.
- (40) Ezratty, E. J.; Bertaux, C.; Marcantonio, E. E.; Gundersen, G. G. Clathrin mediates integrin endocytosis for focal adhesion disassembly in migrating cells. *J. Cell Biol.* **2009**, *187* (5), 733–747.

- (41) Wu, X.; Zhao, X.; Baylor, L.; Kaushal, S.; Eisenberg, E.; Greene, L. E. Clathrin exchange during clathrin-mediated endocytosis. *J. Cell Biol.* **2001**, *155* (2), 291–300.
- (42) Rappoport, J. Z.; Simon, S. M. Real-time analysis of clathrin-mediated endocytosis during cell migration. *J. Cell Sci.* **2003**, *116* (5), 847–855.
- (43) Howes, M. T.; Kirkham, M.; Riches, J.; Cortese, K.; Walser, P. J.; Simpson, F.; Hill, M. M.; Jones, A.; Lundmark, R.; Lindsay, M. R.; Hernandez-Deviez, D. J.; Hadzic, G.; McCluskey, A.; Bashir, R.; Liu, L.; Pilch, P.; McMahon, H.; Robinson, P. J.; Hancock, J. F.; Mayor, S.; Parton, R. G. Clathrin-independent carriers form a high capacity endocytic sorting system at the leading edge of migrating cells. *J. Cell Biol.* **2010**, *190* (4), 675–691.
- (44) Ehrlich, M.; Boll, W.; Van Oijen, A.; Hariharan, R.; Chandran, K.; Nibert, M. L.; Kirchhausen, T. Endocytosis by random initiation and stabilization of clathrin-coated pits. *Cell* **2004**, *118* (5), 591–605.
- (45) Loerke, D.; Mettlen, M.; Yarar, D.; Jaqaman, K.; Jaqaman, H.; Danuser, G.; Schmid, S. L. Cargo and dynamin regulate clathrin-coated pit maturation. *PLoS Biol.* **2009**, *7* (3), e57.
- (46) Rappoport, J. Z.; Taha, B. W.; Lemeer, S.; Benmerah, A.; Simon, S. M. The AP-2 complex is excluded from the dynamic population of plasma membrane-associated clathrin. *J. Biol. Chem.* **2003**, *278* (48), 47357–47360.
- (47) Merrifield, C. J.; Feldman, M. E.; Wan, L.; Almers, W. Imaging actin and dynamin recruitment during invagination of single clathrin-coated pits. *Nat. Cell Biol.* **2002**, *4* (9), 691–698.
- (48) Merrifield, C. J.; Perrais, D.; Zenisek, D. Coupling between clathrin-coated-pit invagination, cortactin recruitment, and membrane scission observed in live cells. *Cell* **2005**, *121* (4), 593–606.
- (49) Lee, D. W.; Wu, X.; Eisenberg, E.; Greene, L. E. Recruitment dynamics of GAK and auxilin to clathrin-coated pits during endocytosis. *J. Cell Sci.* **2006**, *119* (17), 3502–3512.
- (50) Rappoport, J. Z.; Kemal, S.; Benmerah, A.; Simon, S. M. Dynamics of clathrin and adaptor proteins during endocytosis. *American Journal of Physiology. Cell Physiology* **2006**, *291* (5), C1072–81.
- (51) Shimada, A.; Niwa, H.; Tsujita, K.; Suetsugu, S.; Nitta, K.; Hanawa-Suetsugu, K.; Akasaka, R.; Nishino, Y.; Toyama, M.; Chen, L.; Liu, Z. J.; Wang, B. C.; Yamamoto, M.; Terada, T.; Miyazawa, A.; Tanaka, A.; Sugano, S.; Shirouzu, M.; Nagayama, K.; Takenawa, T.; Yokoyama, S. Curved EFC/F-BAR-domain dimers are joined end to end into a filament for membrane invagination in endocytosis. *Cell* **2007**, *129* (4), 761–772.
- (52) Yarar, D.; Waterman-Storer, C. M.; Schmid, S. L. A dynamic actin cytoskeleton functions at multiple stages of clathrin-mediated endocytosis. *Mol. Biol. Cell* **2004**, *16* (2), 964–975.
- (53) Saffarian, S.; Cocucci, E.; Kirchhausen, T. Distinct dynamics of endocytic clathrin-coated pits and coated plaques. *PLoS Biol.* **2009**, *7* (9), e1000191.
- (54) Cossart, P.; Lebreton, A. A trip in the "New Microbiology" with the bacterial pathogen *Listeria monocytogenes*. *FEBS Lett.* **2014**, *588* (15), 2437–45.
- (55) Veiga, E.; Cossart, P. *Listeria* hijacks the clathrin-dependent endocytic machinery to invade mammalian cells. *Nat. Cell Biol.* **2005**, *7* (9), 894–900.
- (56) Veiga, E.; Cossart, P. The role of clathrin-dependent endocytosis in bacterial internalization. *Trends Cell Biol.* **2006**, *16* (10), 499–504.
- (57) Pizarro-Cerda, J.; Bonazzi, M.; Cossart, P. Clathrin-mediated endocytosis: what works for small, also works for big. *BioEssays* **2010**, *32* (6), 496–504.